

Observational Studies of Pre-Stellar Cores and Infrared Dark Clouds

Paola Caselli¹

¹School of Physics and Astronomy, University of Leeds, Leeds LS2 9JT, UK
email: p.caselli@leeds.ac.uk

Abstract. Stars like our Sun and planets like our Earth form in dense regions within interstellar molecular clouds, called pre-stellar cores (PSCs). PSCs provide the initial conditions in the process of star and planet formation. In the past 15 years, detailed observations of (low-mass) PSCs in nearby molecular cloud complexes have allowed us to find that they are cold ($T < 10$ K) and quiescent (molecular line widths are close to thermal), with a chemistry profoundly affected by molecular freeze-out onto dust grains. In these conditions, deuterated molecules flourish, becoming the best tools to unveil the PSC physical and chemical structure. Despite their apparent simplicity, PSCs still offer puzzles to solve and they are far from being completely understood. For example, what is happening to the gas and dust in their nuclei (the future stellar cradles) is still a mystery that awaits for ALMA. Other important questions are: how do different environments and external conditions affect the PSC physical/chemical structure? Are PSCs in high-mass star forming regions similar to the well-known low-mass PSCs? Here I review observational and theoretical work on PSCs in nearby molecular cloud complexes and the ongoing search and study of massive PSCs embedded in infrared dark clouds (IRDCs), which host the initial conditions for stellar cluster and high-mass star formation.

Keywords. astrochemistry; line: profiles; molecular data; molecular processes; radiative transfer; stars: formation; ISM: clouds, dust, extinction, kinematics and dynamics, molecules.

1. Introduction

For about 30 years we have known that stars like our Sun form within the dense regions of interstellar molecular clouds (e.g. Benson & Myers 1989; Beichman *et al.* 1986), where submicron sized dust grains and molecules such as H_2 , CO and more complex organic species coexist and interact (Herbst & van Dishoeck 2009). These regions are called dense cores (Myers *et al.* 1983) and represent the initial conditions of the star formation process (e.g. Shu *et al.* 1987). In fact, observations in quiescent regions, such as the Pipe nebula (Alves *et al.* 2007; Rathborne *et al.* 2009) and the Aquila Rift (André *et al.* 2010; Könyves *et al.* 2010) indicate that the stellar mass function is the reflection of the core mass function (CMF). If so, processes controlling the formation of the cores sets the initial mass function (IMF; Salpeter 1955). Observations of dense cores and their interpretation are therefore fundamental to put constraints on star and planet formation theory as well as on simulations of molecular cloud formation and evolution. How can we study the initial conditions of star and planet formation by looking at dense cores?

The initial conditions are soon lost as dense cores become associated with protostars, which drive powerful outflows and alter the physical and chemical properties of the parent cloud (e.g. Arce *et al.* 2007, 2010; Foster *et al.* 2009; Friesen *et al.* 2010a; Pineda *et al.* 2011). Thus one first needs to identify dense cores on the verge of star formation, the so-called pre-stellar cores (PSCs). PSCs are typically cold (temperature ≤ 10 K) and have volume densities $> \approx 2 \times 10^{-19} \text{ g cm}^{-3}$, or number densities $> 5 \times 10^4 \text{ H}_2$ molecules per cc (e.g. Ward-Thompson *et al.* 1994; Crapsi *et al.* 2005). In such environments, the

dust mostly emits sub-millimetre radiation (peaking around $300\mu\text{m}$), and the rotational transitions of molecules such as CO emit in the readily accessible millimetre spectrum. While CO is the most abundant molecule after H_2 , there are a host of other observable molecules that provide additional information. For example, ammonia (NH_3 ; e.g. Goodman *et al.* 1993) and dyazenilium (N_2H^+ ; Caselli *et al.* 1995, 2002a) both have lower optical depths and are better tracers of dense gas. Both molecules have hyperfine spectra useful in determining the gas temperature and column densities. Over the past 15 years, observations of dust, CO, NH_3 , and N_2H^+ have established the basic structure of the cores: nearly hydrostatic equilibrium and heated from the outside by starlight. More recent studies have been able to analyze observations within this basic framework to deduce some of the physical and chemical processes in molecular clouds such as internal wave motions, UV heating, molecular depletion and desorption between gas and solid phases, and chemical fractionation. In Sect. 2 below we discuss this further. The more recent study of PSCs in high-mass star forming regions is described in Sect. 3.

2. Low-mass PSCs

The state of the art in the PSCs field is summarized below. More comprehensive reviews can be found in Di Francesco *et al.* (2007) and Bergin & Tafalla (2007).

2.1. Molecular freeze-out

First identified by Ward-Thompson *et al.* (1994) as centrally concentrated cores in the dust millimetre continuum emission, PSCs are characterized by relatively large central number densities (a few $\times 10^6 \text{ cm}^{-3}$), low central kinetic temperature ($T \simeq 6 \text{ K}$; Crapsi *et al.* 2007), and kinematic features which can be reproduced by gravitational collapse motions (e.g. Caselli *et al.* 2002b; van der Tak *et al.* 2005). CO molecules (typically used to derive cloud masses, assuming a canonical CO/ H_2 abundance ratio of $\simeq 10^{-4} \text{ cm}^{-3}$, as measured in nearby molecular clouds; e.g. Frerking *et al.* 1987, Pineda *et al.* 2008) do not trace the dust peak at all (Willacy *et al.* 1998; Caselli *et al.* 1999; Bacmann *et al.* 2002; Pagani *et al.* 2007). To reproduce observations toward the PSC L1544, about 90% of CO molecules should leave the gas phase, on average along the line of sight, and over 99% of them must deplete in the core nucleus (Caselli *et al.* 1999). The only easy way to get rid of gas-phase molecules in quiescent and cold regions is to deposit them on the surface of dust particles, forming thick icy mantles (e.g. Leger 1983; Lacy *et al.* 1994; Ossenkopf & Henning 1994; Ormel *et al.* 2009; Chiar *et al.* 2011).

Unlike CO and other C-bearing species (Tafalla *et al.* 2006), N-bearing molecules do not significantly freeze-out in PSC centers (Hily-Blant *et al.* 2010): only a factor $\simeq 2$ abundance drop for N_2H^+ (Caselli *et al.* 2002c, Bergin *et al.* 2002) and hints of abundance rise for NH_3 (Tafalla *et al.* 2004). This is a puzzle in regions where CO is heavily depleted, given that the binding energy of N_2 (the precursor of N_2H^+ and NH_3) onto bare grains and icy surfaces is similar to the CO binding energy (Öberg *et al.* 2005) and the sticking coefficient is the same for the two species ($\simeq 1$; Bisschop *et al.* 2006). Also, NH_3 is significantly more strongly bound on grain mantles than CO. A possible explanation may be the slow conversion of atomic nitrogen into N_2 , because of the slow neutral-neutral reactions involved in the process (Hily-Blant *et al.* 2010), the possibly low sticking probability of N ($\simeq 0.1$; Flower *et al.* 2006) and the fact that the freeze-out of CO decreases the destruction rate of N_2H^+ and molecular ions important for the formation of NH_3 (such as NH^+ ; see also Aikawa *et al.* 2005, 2008). Indeed, Maret *et al.* (2006) found evidence of a low fraction of N_2 ($\simeq 10^{-6}$ with respect to H nuclei) and a consequent high N/ N_2 ratio toward the starless core B68, although some N has

to be trapped on the surface of dust grains to avoid a too efficient production of N_2 . Interestingly, Hily-Blant *et al.* (2010) also require a low fractional abundance of atomic nitrogen in the gas phase ($\leq 10^{-6}$), to reproduce the observed abundance ratio of N-bearing species tracing the CO-depleted zone of five starless cores (but uncertainties on the rate coefficients of key neutral-neutral reactions prevent unambiguous conclusions). In any case, in the central few hundred AU of a PSC (the PSC nucleus), where the volume density is $>10^6 \text{ cm}^{-3}$, molecules freeze-out onto dust grains with time scales $\leq 10^3/[n(\text{H}_2)/10^6 \text{ cm}^{-3}] \text{ yr}$ (assuming a gas-to-dust mass ratio of 100 and a dust grain radius of $0.1 \mu\text{m}$; e.g. van Dishoeck *et al.* 1993, Flower *et al.* 2005), and no high density tracer is expected to survive in the gas phase (except for those molecules composed by the volatile light elements H and D, such as H_3^+ and its deuterated isotopologues; see Sect. 2.2). An example of this is provided by the recent interferometric observations of $\text{N}_2\text{H}^+(1-0)$ toward Oph B (Friesen *et al.* 2010b), where no emission was found toward dust continuum peaks within the core.

Keto & Caselli (2008, 2010) used the basic temperature-density model to predict line intensities and profiles for different values of the cosmic ray ionization rate and the reverse process to depletion, molecular desorption, which is dependent on cosmic rays. Detailed comparison with observed molecular lines put limits on the rate of cosmic-ray ionization ($\simeq 1 \times 10^{-17} \text{ s}^{-1}$) and desorption (about 30 times larger than the value deduced by Hasegawa & Herbst 1993 and in agreement with more recent studies by Branga & Johnson 2004 and Herbst & Cuppen 2006). Moreover, to reproduce the low temperature observed toward the core nucleus ($\simeq 6 \text{ K}$) the dust opacity has to increase by a factor of about 4 compared to the standard dust opacities of Ossenkopf & Henning (1994). This is consistent with fluffy dust, suggesting that dust grains have started to coagulate (see also Ormel *et al.* 2009), with a consequent reduction of the molecular freeze-out rate because of the smaller surface area available for adsorption (Flower *et al.* 2005).

2.2. Deuterium fractionation

Deuterated molecules are highly enhanced in PSC nuclei. The reason for this is briefly outlined here. In cold and dark clouds (such as PSCs), H_2 molecules are mainly destroyed by cosmic rays, which produce H_2^+ . As soon as H_2^+ is formed, it reacts with another H_2 molecule, forming one of the most important molecular ions in astrochemistry: H_3^+ . This molecular ion can easily cede a proton to atoms and other species, starting astrochemical processes and increasing the molecular complexity in the interstellar medium. H_3^+ can also exchange its proton with a deuteron, through the reaction: $\text{H}_3^+ + \text{HD} \rightarrow \text{H}_2\text{D}^+ + \text{H}_2 + \Delta E$ ($\Delta E = 230 \text{ K}$; Millar *et al.* 1989). If the gas temperature is below 20 K , such as in PSCs, the above exothermic reaction can only proceed from left to right, enhancing the $\text{H}_2\text{D}^+ / \text{H}_3^+$ abundance ratio. This is reflected in species (such as DCO^+ and N_2D^+), which form in reactions of neutrals (CO and N_2 , respectively) with H_2D^+ . The ratio between deuterated and non-deuterated species (e.g. $\text{N}_2\text{D}^+ / \text{N}_2\text{H}^+$) is called D-fraction (R_{D}) and its values can be as large as a few %, about 3 orders of magnitude larger than the cosmic D/H ratio ($\simeq 10^{-5}$; e.g. Linsky *et al.* 2006).

R_{D} increases even farther (to about 13 orders of magnitude in multiply deuterated species; e.g. Ceccarelli *et al.* 2007) if the abundance of the main destruction partners of H_3^+ and H_2D^+ (mainly CO and O) is reduced, e.g. via freeze-out. This was predicted by Dalgarno & Lepp (1984) and observationally proved toward several starless cores and PSCs (Caselli *et al.* 2002c; Bacmann *et al.* 2003). Crapsi *et al.* (2005) found criteria to identify PSCs among starless cores by measuring R_{D} and studying line profiles: PSCs have (i) high R_{D} ($> 10\%$); (ii) large amount of CO freeze-out ($> 99\%$); (iii) large central density ($> 5 \times 10^5 \text{ cm}^{-3}$) and centrally concentrated density profile; (iv) kinematics consistent with

central gravitational infall. This is important because PSCs, the future stellar cradles, are the best candidates where to find the initial conditions in the process of star formation. Starless cores with lower densities and shallower density profiles may oscillate around an equilibrium configuration (e.g. Lada *et al.* 2003) or expand and disperse.

The large amount of molecular freeze-out and the consequent boost in the D-fraction explain why PSCs are the strongest emitters of H_2D^+ and D_2H^+ in the Galaxy (Caselli *et al.* 2003, 2008; Vastel *et al.* 2004). To reproduce these observations, chemical models had to include multiply deuterated species (Roberts *et al.* 2003). Being bright (main beam brightness temperatures $\simeq 1$ K), the ortho- H_2D^+ ($1_{1,0}-1_{1,1}$) line is an ideal tracer of PSC nuclei, even in those regions where most of the heavier species are gone from the gas phase (the “complete depletion” zone; Walmsley *et al.* 2004). The emission of ortho- H_2D^+ extends over sizes $\simeq 5,000$ AU toward L1544 (Vastel *et al.* 2006), similar to the para- D_2H^+ ($1_{1,0}-1_{0,1}$) line (Parise *et al.* 2011). This is the size of the “deuteration zone”, where CO is mostly frozen onto dust grains and bright lines of N_2D^+ and deuterated ammonia can be observed (e.g. Crapsi *et al.* 2005, 2007). Caselli *et al.* (2008) extended the search of ortho- H_2D^+ in a sample of PSCs and cores with embedded protostars. Variations in the amount of R_{D} and ortho- H_2D^+ column densities were correlated with physical parameters and found that large uncertainties in the interpretation were present, due to our poor knowledge of the cosmic-ray ionization rate (Dalgarno 2006), the dust grain size distribution (Ormel *et al.* 2009), the H_2 ortho-to-para ratio (Troscompt *et al.* 2009; Pagani *et al.* 2009) and the abundance of atomic oxygen in molecular clouds and dense cores (Melnick & Bergin 2005). Caselli *et al.* (2008) suggested that an important source of the scatter observed in the correlation plots is probably due to variations in the ortho-to-para ratio of H_2D^+ , from >0.5 for PSCs, with gas temperatures <10 K, to 0.03 for protostellar cores, consistent with chemical models of dense cores with temperature $\simeq 15$ K gas (Flower *et al.* 2004; see also Emprechtinger *et al.* 2009 and Friesen *et al.* 2010a for further discussion on the variation of deuterium fractionation toward protostellar objects).

2.3. Physical Structure

Measurements of dust and gas temperature profiles (Crapsi *et al.* 2007; Pagani *et al.* 2007), as well as estimates of their density structure, kinematics, chemical composition and ionization fraction (e.g. Caselli *et al.* 2002b; Bergin *et al.* 2002; Schnee *et al.* 2007; Keto & Caselli 2008, 2010) provided the following conclusions: (i) PSCs are mainly thermally supported (with some additional energy furnished by waves and subsonic turbulence; e.g. Caselli *et al.* 2002a; Lada *et al.* 2008). (ii) Subsonic oscillations and large scale wave motions are important to PSC internal energy (Keto & Field 2005; Broderick *et al.* 2008); (iii) PSCs are heated from outside by starlight and throughout by cosmic rays (e.g. Evans *et al.* 2001; Zucconi *et al.* 2001); (iv) main coolants are molecular line radiation (in particular CO) in the outer regions and dust in the central nuclei (e.g. Goldsmith 2001; Galli *et al.* 2002); (v) their density structure is set by the Lane-Emden equation (e.g. Alves *et al.* 2001); (vi) the molecular abundance across PSCs is set by freeze-out/desorption processes in the core centers and by photodissociation in the outskirts (Pavlyuchenkov *et al.* 2008; Keto & Caselli 2008); (vii) PSCs are thermally supercritical cloud cores (Keto & Caselli 2008), with infall velocities of $\simeq 0.1$ km s $^{-1}$ peaking at $\simeq 1000$ AU from the core center (Keto & Caselli 2010).

High angular resolution observations (probing linear sizes of $\simeq 800$ AU) using the Very Large Array (VLA) and the Plateau de Bure Interferometer (PdBI) have shown that the specific angular momentum of the PSC L1544 drops from $\simeq 5 \times 10^{21}$ cm 2 s $^{-1}$ at sizes of 0.04 (traced by NH_3) to $\simeq 3.5 \times 10^{20}$ cm 2 s $^{-1}$ at sizes of 0.001 pc (traced by NH_2D ; Crapsi

et al. 2007). While the former value is typical of starless cores (e.g. Ohashi *et al.* 1999), the smaller obtained toward the core nucleus resembles values measured toward protostellar envelopes and it is consistent with what found in more evolved objects (Belloche *et al.* 2002). ALMA will allow us to dive into the central few thousands AU and study the physical conditions and kinematics of the core nucleus, the future protostar and protoplanetary disk cradle.

Figure 1 shows a schematic summary of the physical and chemical structure of a representative PSC based on recent observational and theoretical work. The panel is divided in five regions with different gray scales, representing various chemical zones: (i) the “complete depletion” zone ($r \leq 1000$ AU, $A_V \geq 60$ mag), not yet discovered but predicted by chemical models (e.g. Walmsley *et al.* 2004). Here, the main tracers of the gas are expected to be the ortho- H_2D^+ ($1_{1,0}-1_{1,1}$) and para- D_2H^+ ($1_{1,0}-1_{0,1}$), both observable with ALMA. (ii) The “depletion zone” ($1000 < r \leq 5,000$ AU, $A_V \geq 20$ mag), where the peak of deuterated molecules such as N_2D^+ , D_2CO and deuterated ammonia are found (e.g. Caselli *et al.* 2002a; Bacmann *et al.* 2003; Crapsi *et al.* 2007). Other non-deuterated molecules more resistant than CO to the freeze-out have also been observed in the same region: CN, HCN, HNC (Hily-Blant *et al.* 2010, see also Tafalla *et al.* 2006). (iii) The “CO freeze-out zone” ($r \leq 7,000$ AU, $A_V \geq 5$ mag) where the majority of CO molecules (>99%, Caselli *et al.* 1999) are locked onto icy dust grain mantles. (iv) The “dark-cloud chemistry zone” ($7,000 < r \leq 15,000$ AU, $A_V \geq 4$ mag), traced by CO molecules and higher density tracers chemically linked to CO, such as HCO^+ . Because carbon atoms are probably not completely locked into CO molecules (due to the presence of interstellar UV photons), carbon-chain species such as CCS and CCH (Tafalla *et al.* 2006; Padovani *et al.* 2009) can also be found here. (v) The “photodissociation region” (PDR; e.g. Kaufman *et al.* 1999), where FUV ($6\text{eV} < h\nu < 13.6\text{eV}$) photons play a crucial role in the chemistry, dissociating molecules and maintaining most of the carbon and oxygen in atomic form in the gas phase. The detailed structure of PSCs of course depends on the environment, so that the size and physical/chemical properties of the various PSC layers are expected to change in different molecular cloud complexes or in more massive star forming regions. Understanding how external conditions affect the structure of PSCs is crucial to shed light on the star formation process in different environments.

2.4. The water content

Oxygen is the third most abundant element in the Universe and it has a crucial role in the chemical and physical structure of molecular clouds, where large fractions are locked into CO and H_2O molecules. Unfortunately, large uncertainties in the chemistry of oxygen are still present due to the difficulty of observing H_2O and O in molecular clouds. In dark ($A_V > 4$ mag) clouds, H_2O is thought to be mostly in solid form (Hollenbach *et al.* 2009), in agreement with the stringent upper limits on the ortho- H_2O ($1_{1,0}-1_{0,1}$) obtained toward dark clouds and dense cores ($x(\text{H}_2\text{O}) \equiv N(\text{H}_2\text{O})/N(\text{H}_2) < 3 \times 10^{-8}$, 8×10^{-9} and 7×10^{-9} toward B68, Oph D and Cha-MMS1, respectively; Bergin & Snell 2002; Klotz *et al.* 2008). These limits are however difficult to interpret, given that radiative transfer modeling has shown that line trapping and absorption of the dust continuum can heavily affect the water emission from dense interstellar clouds (Poelman *et al.* 2007). Moreover, a significant fraction of atomic oxygen can still be maintained in the gas phase, thanks to non-thermal (e.g. cosmic-ray induced) desorption processes (Caselli *et al.* 2002c), as in fact measured with ISO (Infrared Space Observatory) toward two molecular clouds (Caux *et al.* 1999; Vastel *et al.* 2000).

The superior angular resolution and sensitivity of the Herschel Space Observatory (Pilbratt *et al.* 2010) has recently furnished the first column density measure of ortho- H_2O

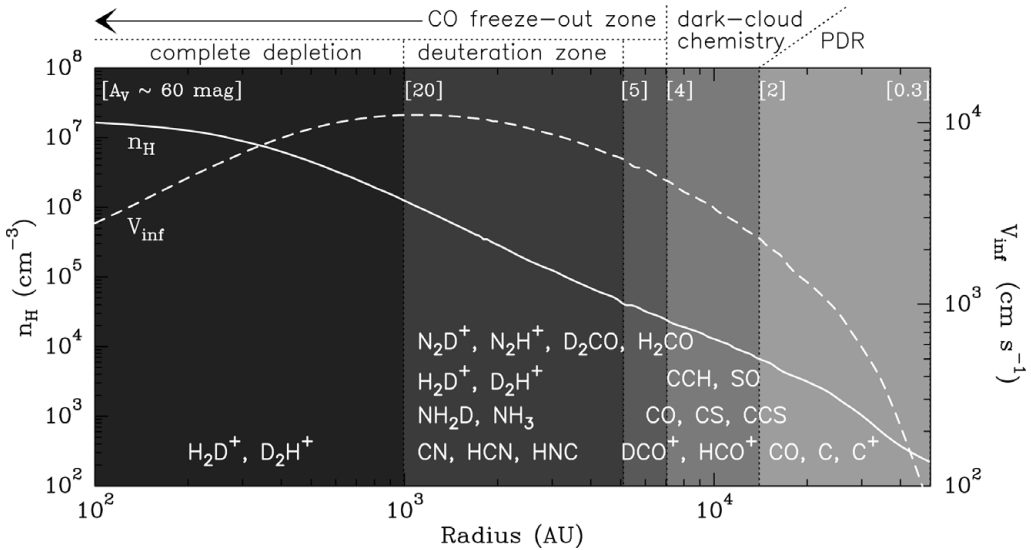


Figure 1. Schematic representation of the physical and chemical structure of a PSC in a low-mass star forming region, based on detailed observations and hydrodynamic/radiative transfer modeling of the PSC L1544, isolated PSC embedded in the Taurus molecular cloud complex. The white curves represent the hydrogen nuclei volume density (n_{H} ; solid, left labels) and the infall velocity (V_{inf} ; dashed, right labels) profiles as derived by Keto & Caselli (2010). The density is predicted to be $2 \times 10^7 \text{ cm}^{-3}$ within the central 500 AU. The infall velocity has a peak of $\simeq 0.1 \text{ km s}^{-1}$ around 1,000 AU. The panel is divided in five regions with different gray scales, representing various chemical zones (see text).

toward the PSC L1544 (Caselli *et al.* 2010, see Figure 2), within the WISH (Water In Star-forming regions with Herschel, van Dishoeck *et al.* 2011) guaranteed time programme. No water line was detected toward the starless core B68 (from which a stringent upper limit of the water abundance was deduced: $x(\text{ortho} - \text{H}_2\text{O}) < 1.3 \times 10^{-9}$). The water detection toward L1544 has been possible because L1544, unlike B68, is centrally concentrated and thus has a relatively bright FIR nucleus (about 5 Jy at 557 GHz within the Herschel beam of $40''$). In fact, the ortho- $\text{H}_2\text{O}(1_{1,0}-1_{0,1})$ line has been detected in *absorption* at a 5σ level (Figure 2). The column density is $N(\text{ortho} - \text{H}_2\text{O}) \simeq 8 \times 10^{12} \text{ cm}^{-2}$. Using the H_2 column density deduced by the 1.3 mm dust continuum emission (Ward-Thompson *et al.* 1999; Figure 2) within the Herschel beam, Caselli *et al.* (2010) found $x(\text{ortho} - \text{H}_2\text{O}) \simeq 2 \times 10^{-10}$ toward the central few thousand AUs, where CO is highly frozen onto dust grains. This value is close to that measured in the envelope of massive young stellar objects (van der Tak *et al.* 2010). Radiative transfer models of collapsing Bonnor-Ebert spheres with the inclusion of simplified chemistry based on the Hollenbach *et al.* (2009) model, were able to reproduce the observations assuming a peak abundance of water vapor of $\simeq 10^{-8}$ at 0.1 pc from the PSC center. Higher gas phase abundance of water are ruled out because the predicted absorption is too strong. These observations have been recently repeated and the S/N significantly improved so that a more detailed analysis and comparison with chemical models is now possible and will soon be presented (Caselli *et al.* 2011, in prep.).

Figure 2 shows the ortho- $\text{H}_2\text{O}(1_{1,0}-1_{0,1})$ spectrum toward L1544 as presented in Caselli *et al.* (2010), where a comparison with the CO(1-0) profiles is also given. It is interesting

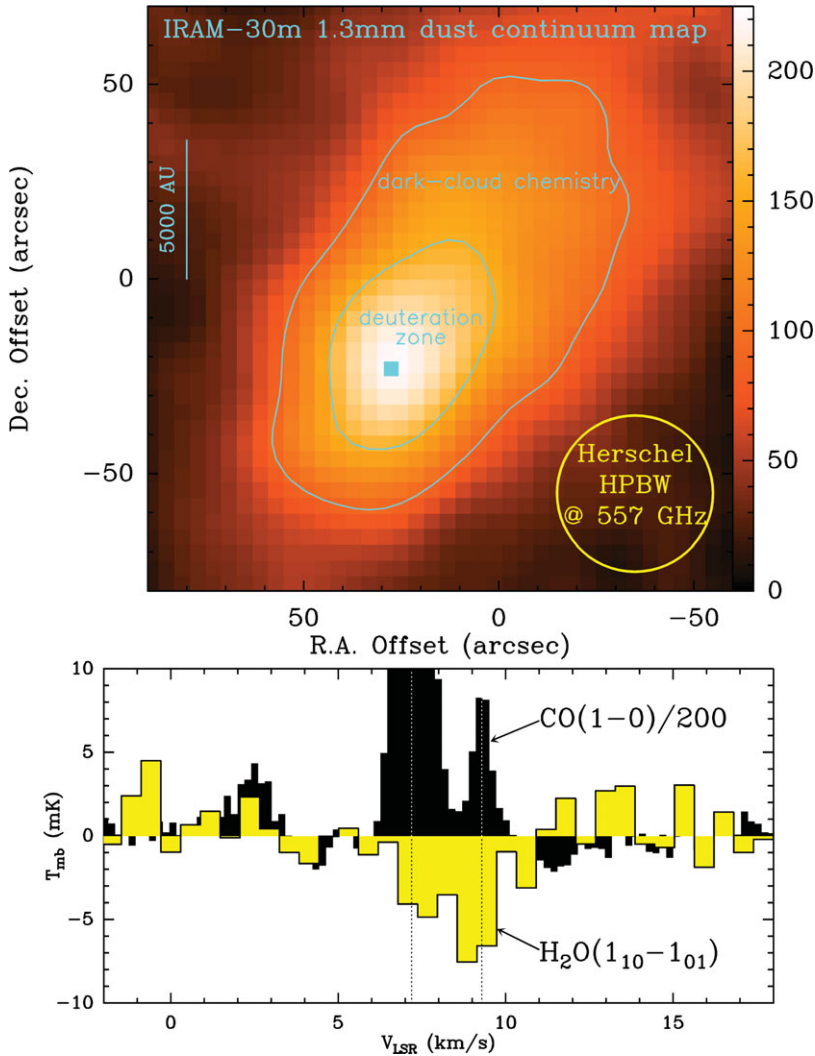


Figure 2. (Top panel) The 1.3 mm dust continuum emission map obtained at the IRAM-30m antenna by Ward-Thompson *et al.* (1999), smoothed at 22'' resolution to improve the sensitivity. The wedge on the right is in units of mJy/22''-beam. The contours represent the 50% and 70% of the dust continuum peak (225 mJy/beam). They approximately coincide with the size of the “dark-cloud chemistry” zone and “deuteration zone”, respectively (see Figure 1). The square locate the dust peak position, observed by Herschel (RA(J2000) = 05^h 04^m 17.21^s, Dec(J2000) = 25^{deg} 10' 42.8''). The Herschel beam at 557 GHz is the circle at the bottom-right corner. (Bottom panel) The feature in absorption is the ortho-H₂O(1_{1,0}-1_{0,1}) line observed against the 11 mK continuum emission of the dust at the same frequency (from Caselli *et al.* 2010). The black histogram is the CO(1-0) line (scaled down by a factor of 200) observed with the Five College Radio Astronomy Observatory (FCRAO).

to see that the water absorption is present in the same velocity range of the CO(1-0) emission line, including the faint CO component redshifted by about 2 km s⁻¹ away from the centroid velocity of the L1544 dense gas tracers. These are the first observations of water vapor in dark clouds and they are crucial to shed light on the oxygen chemistry and the formation of water vapor in quiescent regions.

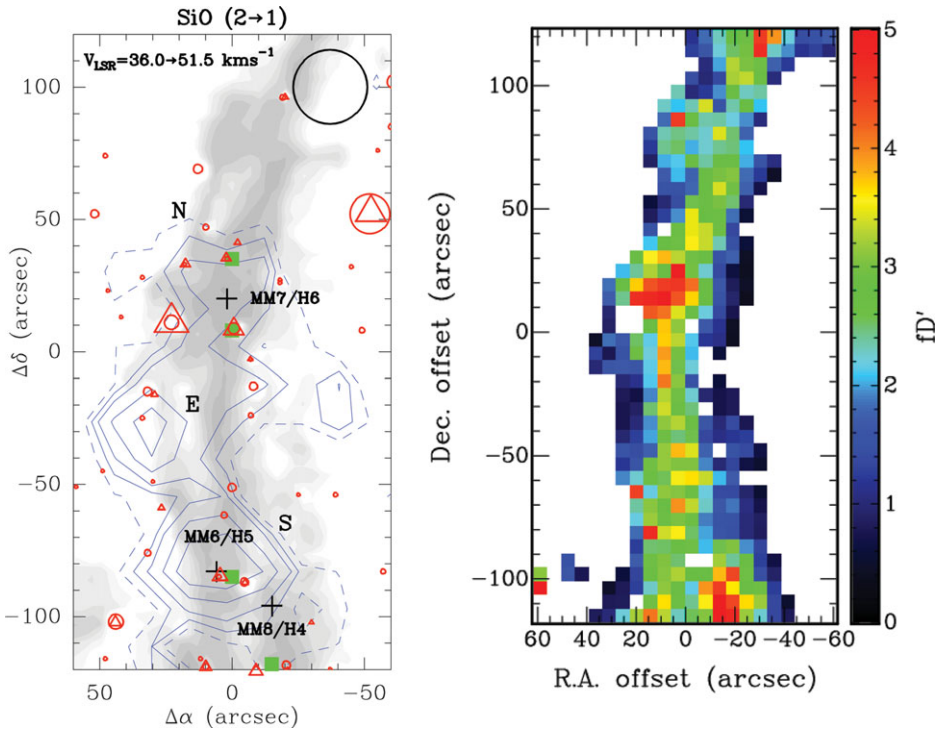


Figure 3. (Left panel) Integrated intensity map of the SiO (2-1) line towards G035.39-00.33 (blue contours), overlapped on the mass surface density map of Butler & Tan (2009, grey scale). The contour levels of the SiO emission are 10 (2σ ; dashed contour), 15, 20, 30 and 40 mK km s^{-1} . For the mass surface density map, contours are 0.014 (2σ), 0.021, 0.035, 0.049, 0.07, 0.105 and 0.14 g cm^{-2} . Crosses indicate the cores found by Rathborne *et al.* (2006). Red open circles, red open triangles and green squares show the location of the 8- and 24- μm sources and 4.5- μm extended emission, respectively. The marker sizes used for the 8- and 24- μm sources have been scaled by the source flux. The SiO (2-1) beam size is plotted at the upper-right corner (adapted from Jimenez-Serra *et al.* 2010). (Right panel) CO depletion factor map (from Hernandez *et al.* 2011) of G035.39-00.33. The abundance of CO decreases by factors 3-5 in the highest extinction regions, indicating the presence of cold dust ($T < 20\text{ K}$) and consequent CO freeze-out.

3. Massive PSCs

The majority of stars form in clusters within giant molecular clouds (GMCs; e.g. Lada & Lada 2003), so it is crucial to understand how stellar clusters form. However, the initial conditions in the process of high-mass star and stellar cluster formation are still highly debated. Understanding what causes a particular region of a GMC to attain high densities on the way to forming a star cluster is a major open question in the fields of star and galaxy formation. There are two main classes of theories: spontaneous gravitational instability perhaps regulated by photo-ionization (McKee 1989) or turbulence (Krumholz & McKee 2005) and triggering by some external process, such as HII regions (Deharveng *et al.* 2005), supernova blastwaves (Palous *et al.* 1994), turbulent motions (MacLow & Klessen 2004) or GMC collisions (Tan 2000). Detailed studies of the chemical/physical structure and kinematics of massive PSCs (MPSCs) and comparison with the properties of low-mass PSCs (see Sect. 2) are sorely needed.

The search and study of MPSCs in high-mass star forming regions is however at its infancy, given that it is challenged by the MPSC short time scales, large distances and their proximity to active sites of high-mass star and cluster formation, which can affect their

dynamical evolution. For these reasons, the initial conditions in the process of high-mass and stellar cluster formation require the search for relatively quiescent massive clouds and then study the embedded stellar population content to identify starless regions, possibly away from the reach of powerful outflows driven by massive young stellar objects (MYSO) embedded in nearby clumps. The best candidates to host *pristine* MPSCs are the so-called infrared dark clouds (IRDCs; e.g. Beuther *et al.* 2007; Zhang *et al.* 2009), in particular those with a relatively large fraction of quiescent gas (i.e. low star formation activity) and filamentary structures, which are predicted to be the initial morphologies of GMCs in several classes of dynamical formation models (e.g. van Loo *et al.* 2007; Heitsch *et al.* 2009).

IRDCs are high extinction regions viewed against the diffuse mid-IR Galactic background (P  rault *et al.* 1996; Egan *et al.* 1998; Peretto & Fuller 2009). They have very high-mass surface densities that are similar to known regions of massive star and star cluster formation (Tan 2005). They are cold (temperatures between 8 and 20 K; Pillai *et al.* 2006; Peretto *et al.* 2010; Stamatellos *et al.* 2010; Devine *et al.* 2011; Ragan *et al.* 2011), host clumps with densities $\simeq 10^4$ - 10^6 cm⁻³ (Teyssier *et al.* 2002; Butler & Tan 2009; Swift 2009; Zhang *et al.* 2011), show chemical compositions similar to low-mass PSCs (Vasyunina *et al.* 2011), including large deuterium fractions R_D (Pillai *et al.* 2007; Chen *et al.* 2010). In fact, Fontani *et al.* (2011) have found significantly larger N_2D^+/N_2H^+ column density ratios toward a sample of high mass starless cores (HMSCs) embedded in cold IRDCs (between 0.3 and 0.7) than the rest of their sample, which includes HMSCs embedded in more active high-mass star forming regions as well as clumps associated with high-mass protostellar objects and ultra-compact HII (UCHII) regions. Thus, R_D measurements are powerful tools to identify MPSCs among the IRDC starless cores, which are now readily found by Herschel on a galactic scale (e.g. Molinari *et al.* 2010; Wilcock *et al.* 2010; Henning *et al.* 2010).

Detailed mapping and analysis has been recently done (and more it is under way) of a highly filamentary IRDC: G035.39-00.33. This region (i) has one of the most extreme filamentary structure in the Rathborne *et al.* (2006) sample of IRDCs studied in the mm continuum emission; (ii) shows extended quiescent regions with high-mass surface density and relatively low star formation activity (as can be seen from the lack of a large population of sources in the Spitzer 24 μ m image, see Figure 3, left panel); (iii) is relatively nearby ($D = 2.9$ kpc). This IRDC overlaps with Spitzer-GLIMPSE data, and is cloud H in the sample of 10 clouds (A-J) studied by Butler & Tan (2009) using extinction mapping in the 8 μ m IRAC band. Hernandez & Tan (2011) have studied the kinematics of the gas associated with this cloud using ¹³CO(1-0) from the Galactic Ring Survey (GRS; Jackson *et al.* 2006) and found evidence for disturbed kinematics, perhaps indicating the filament has formed very recently. Widespread SiO(2-1) emission has been found along the filament, suggestive of a large scale shock caused by the recent collision of molecular filaments, which may have produced the IRDC (Jimenez-Serra *et al.* 2010; Figure 3, left panel). Hernandez *et al.* (2011) have measured significant levels of CO freeze-out (factor of 5; see Figure 3, right panel), indicative of the presence of cold and dense gas. Henshaw *et al.* (2011, in prep) found that the main starless core in IRDC is located at the position where different filaments appear to merge, indicating a recent formation via cloud-cloud collision. The presence of extended SiO emission and CO freeze-out, plus the evidence of filament merging (Henshaw *et al.* 2011, in prep.), further suggest that this region is dynamically young, so it is an ideal target where to study the initial conditions in the process of high-mass star and stellar cluster formation. Higher angular resolution observations are under way to connect the large scale structure of IRDC with the embedded PSCs and clumps. This will allow us to make quantitative comparisons

with models of giant molecular cloud (GMC) formation and evolution (e.g. Heitsch *et al.* 2009, 2011; Butler *et al.*, in prep.), and achieve a deeper understanding of the physical processes involved in the earliest phases of high-mass and cluster forming regions.

Acknowledgements. I am grateful to many collaborators & friends who made all this work possible and very enjoyable, in particular Luca Bizzocchi, Tyler Bourke, Michael Butler, Cecilia Ceccarelli, Antonio Crapsi, Francesco Fontani, Jonathan Henshaw, Audra Hernandez, Itaskun Jiménez-Serra, Eric Keto, Phil Myers, Jaime Pineda, Scott Schnee, Mario Tafalla, Jonathan Tan, Floris van der Tak, Charlotte Vastel, Malcolm Walmsley. A special thank to Audra for her help with Figure 3, and to Mario, Jonathan and Malcolm for their careful reading of the manuscript and important suggestions.

References

- Aikawa, Y., Herbst, E., Roberts, H., & Caselli, P. 2005, *ApJ*, 620, 330
- Aikawa, Y., Wakelam, V., Garrod, R. T., & Herbst, E. 2008, *ApJ*, 674, 984
- Alves, J. F., Lada, C. J., & Lada, E. A. 2001, *Nature*, 409, 159
- Alves, J., Lombardi, M., & Lada, C. J. 2007, *A&A*, 462, L17
- André, P., *et al.*, 2010, *A&A*, 518, L102
- Arce, H. G., Borkin, M. A., Goodman, A. A., Pineda, J. E., & Halle, M. W. 2010, *ApJ*, 715, 1170
- Arce, H. G., Shepherd, D., Gueth, F., Lee, C.-F., Bachiller, R., Rosen, A., & Beuther, H. 2007, *Protostars and Planets V*, 245
- Bacmann, A., Lefloch, B., Ceccarelli, C., Castets, A., Steinacker, J., & Loinard, L. 2002, *A&A*, 389, L6
- Bacmann, A., Lefloch, B., Ceccarelli, C., Steinacker, J., Castets, A., & Loinard, L. 2003, *ApJ*, 585, L55
- Beichman, C. A., Myers, P. C., Emerson, J. P., Harris, S., Mathieu, R., Benson, P. J., & Jennings, R. E. 1986, *ApJ*, 307, 337
- Belloche, A., André, P., Despois, D., & Blinder, S. 2002, *A&A*, 393, 927
- Benson, P. J. & Myers, P. C. 1989, *ApJS*, 71, 89
- Bergin, E. A., Alves, J., Huard, T., & Lada, C. J. 2002, *ApJ*, 570, L101
- Bergin, E. A. & Snell, R. L. 2002, *ApJ*, 581, L105
- Bergin, E. A. & Tafalla, M. 2007, *ARAA*, 45, 339
- Beuther, H., Churchwell, E. B., McKee, C. F., & Tan, J. C. 2007, *Protostars and Planets V*, 165
- Bisschop, S. E., Fraser, H. J., Öberg, K. I., van Dishoeck, E. F., & Schlemmer, S. 2006, *A&A*, 449, 1297
- Bringa, E. M. & Johnson, R. E. 2004, *ApJ*, 603, 159
- Broderick, A. E., Narayan, R., Keto, E., & Lada, C. J. 2008, *ApJ*, 682, 1095
- Butler, M. J. & Tan, J. C. 2009, *ApJ*, 696, 484
- Caselli, P., Benson, P. J., Myers, P. C., & Tafalla, M. 2002a, *ApJ*, 572, 238
- Caselli, P., *et al.*, 2010, *A&A*, 521, L29
- Caselli, P., Myers, P. C., & Thaddeus, P. 1995, *ApJ*, 455, L77
- Caselli, P., van der Tak, F. F. S., Ceccarelli, C., & Bacmann, A. 2003, *A&A*, 403, L37
- Caselli, P., Vastel, C., Ceccarelli, C., van der Tak, F. F. S., Crapsi, A., & Bacmann, A. 2008, *A&A*, 492, 703
- Caselli, P., Walmsley, C. M., Tafalla, M., Dore, L., & Myers, P. C. 1999, *ApJ*, 523, L165
- Caselli, P., Walmsley, C. M., Zucconi, A., Tafalla, M., Dore, L., & Myers, P. C. 2002b, *ApJ*, 565, 331
- Caselli, P., Walmsley, C. M., Zucconi, A., Tafalla, M., Dore, L., & Myers, P. C. 2002c, *ApJ*, 565, 344
- Caux, E., *et al.*, 1999, *A&A*, 347, L1
- Ceccarelli, C., Caselli, P., Herbst, E., Tielens, A. G. G. M., & Caux, E. 2007, *Protostars and Planets V*, 47

- Chen, H.-R., Liu, S.-Y., Su, Y.-N., & Zhang, Q. 2010, *ApJ*, 713, L50
- Chiar, J. E., *et al.*, 2011, *ApJ*, 731, 9
- Crapsi, A., Caselli, P., Walmsley, C. M., Myers, P. C., Tafalla, M., Lee, C. W., & Bourke, T. L. 2005, *ApJ*, 619, 379
- Crapsi, A., Caselli, P., Walmsley, M. C., & Tafalla, M. 2007, *A&A*, 470, 221
- Dalgarno, A. 2006, *Proceedings of the National Academy of Science*, 103, 12269
- Dalgarno, A. & Lepp, S. 1984, *ApJ*, 287, L47
- Devine, K. E., Chandler, C. J., Brogan, C., Churchwell, E., Indebetouw, R., Shirley, Y., & Borg, K. J. 2011, *ApJ*, 733, 44
- Di Francesco, J., Evans, N. J., II, Caselli, P., Myers, P. C., Shirley, Y., Aikawa, Y., & Tafalla, M. 2007, *Protostars and Planets V*, 17
- Deharveng, L., Zavagno, A., & Caplan, J. 2005, *A&A*, 433, 565
- Egan, M. P., Shipman, R. F., Price, S. D., Carey, S. J., Clark, F. O., & Cohen, M. 1998, *ApJ*, 494, L199
- Emprechtinger, M., Caselli, P., Volgenau, N. H., Stutzki, J., & Wiedner, M. C. 2009, *A&A*, 493, 89
- Evans, N. J., II, Rawlings, J. M. C., Shirley, Y. L., & Mundy, L. G. 2001, *ApJ*, 557, 193
- Flower, D. R., Pineau des Forêts, G., & Walmsley, C. M. 2004, *A&A*, 427, 887
- Flower, D. R., Pineau Des Forêts, G., & Walmsley, C. M. 2005, *A&A*, 436, 933
- Flower, D. R., Pineau Des Forêts, G., & Walmsley, C. M. 2006, *A&A*, 456, 215
- Fontani, F., *et al.*, 2011, *A&A*, 529, L7
- Foster, J. B., Rosolowsky, E. W., Kauffmann, J., Pineda, J. E., Borkin, M. A., Caselli, P., Myers, P. C., & Goodman, A. A. 2009, *ApJ*, 696, 298
- Friesen, R. K., Di Francesco, J., Myers, P. C., Belloche, A., Shirley, Y. L., Bourke, T. L., & André, P. 2010a, *ApJ*, 718, 666
- Friesen, R. K., Di Francesco, J., Shimajiri, Y., & Takakuwa, S. 2010b, *ApJ*, 708, 1002
- Frerking, M. A., Langer, W. D., & Wilson, R. W. 1987, *ApJ*, 313, 320
- Galli, D., Walmsley, M., & Gonçalves, J. 2002, *A&A*, 394, 275
- Goldsmith, P. F. 2001, *ApJ*, 557, 736
- Goodman, A. A., Benson, P. J., Fuller, G. A., & Myers, P. C. 1993, *ApJ*, 406, 528
- Hasegawa, T. I. & Herbst, E. 1993, *MNRAS*, 261, 83
- Heitsch, F., Ballesteros-Paredes, J., & Hartmann, L. 2009, *ApJ*, 704, 1735
- Heitsch, F., Naab, T., & Walch, S. 2011, *MNRAS*, 415, 271
- Henning, T., Linz, H., Krause, O., Ragan, S., Beuther, H., Launhardt, R., Nielbock, M., & Vasyunina, T. 2010, *A&A*, 518, L95
- Herbst, E. & Cuppen, H. M. 2006, *Proceedings of the National Academy of Science*, 103, 12257
- Herbst, E. & van Dishoeck, E. F. 2009, *ARAA*, 47, 427
- Hernandez, A. K. & Tan, J. C. 2011, *ApJ*, 730, 44
- Hernandez, A. K., Tan, J. C., Caselli, P., Butler, M. J., Jimenez-Serra, I., Fontani, F., & Barnes, P. 2011, *ApJ*, in press (arXiv:1106.2499)
- Hily-Blant, P., Walmsley, M., Pineau Des Forêts, G., & Flower, D. 2010, *A&A*, 513, A41
- Hollenbach, D., Kaufman, M. J., Bergin, E. A., & Melnick, G. J. 2009, *ApJ*, 690, 1497
- Jiménez-Serra, I., Caselli, P., Tan, J. C., Hernandez, A. K., Fontani, F., Butler, M. J., & van Loo, S. 2010, *MNRAS*, 406, 187
- Kaufman, M. J., Wolfire, M. G., Hollenbach, D. J., & Luhman, M. L. 1999, *ApJ*, 527, 795
- Keto, E. & Caselli, P. 2008, *ApJ*, 683, 238
- Keto, E. & Caselli, P. 2010, *MNRAS*, 402, 1625
- Keto, E. & Field, G. 2005, *ApJ*, 635, 1151
- Klotz, A., Harju, J., Ristorcelli, I., Juvela, M., Boudet, N., & Haikala, L. K. 2008, *A&A*, 492, 767
- Könyves, V., *et al.*, 2010, *A&A*, 518, L106
- Krumholz, M. R. & McKee, C. F. 2005, *ApJ*, 630, 250
- Lacy, J. H., Baas, F., Allamandola, L. J., van de Bult, C. E. P., Persson, S. E., McGregor, P. J., Lonsdale, C. J., & Geballe, T. R. 1984, *ApJ*, 276, 533
- Lada, C. J., Bergin, E. A., Alves, J. F., & Huard, T. L. 2003, *ApJ*, 586, 286

- Lada, C. J., Muench, A. A., Rathborne, J., Alves, J. F., & Lombardi, M. 2008, *ApJ*, 672, 410
- Lada, C. J. & Lada, E. A. 2003, *ARAA*, 41, 57
- Leger, A. 1983, *A&A*, 123, 271
- Linsky, J. L., *et al.*, 2006, *ApJ*, 647, 1106
- Mac Low, M.-M. & Klessen, R. S. 2004, *Reviews of Modern Physics*, 76, 125
- Maret, S., Bergin, E. A., & Lada, C. J. 2006, *Nature*, 442, 425
- McKee, C. F. 1989, *ApJ*, 345, 782
- Melnick, G. J. & Bergin, E. A. 2005, *Advances in Space Research*, 36, 1027
- Millar, T. J., Bennett, A., & Herbst, E. 1989, *ApJ*, 340, 906
- Molinari, S., *et al.*, 2010, *A&A*, 518, L100
- Myers, P. C., Linke, R. A., & Benson, P. J. 1983, *ApJ*, 264, 517
- Öberg, K. I., van Broekhuizen, F., Fraser, H. J., Bisschop, S. E., van Dishoeck, E. F., & Schlemmer, S. 2005, *ApJ*, 621, L33
- Ohashi, N., Lee, S. W., Wilner, D. J., & Hayashi, M. 1999, *ApJ*, 518, L41
- Ormel, C. W., Paszun, D., Dominik, C., & Tielens, A. G. G. M. 2009, *A&A*, 502, 845
- Ossenkopf, V. & Henning, T. 1994, *A&A*, 291, 943
- Padovani, M., Walmsley, C. M., Tafalla, M., Galli, D., & Müller, H. S. P. 2009, *A&A*, 505, 1199
- Pagani, L., Bacmann, A., Cabrit, S., & Vastel, C. 2007, *A&A*, 467, 179
- Pagani, L., *et al.*, 2009, *A&A*, 494, 623
- Palous, J., Tenorio-Tagle, G., & Franco, J. 1994, *MNRAS*, 270, 75
- Parise, B., Belloche, A., Du, F., Güsten, R., & Menten, K. M. 2011, *A&A*, 526, A31
- Pavlyuchenkov, Y., Wiebe, D., Shustov, B., Henning, T., Launhardt, R., & Semenov, D. 2008, *ApJ*, 689, 335
- Perault, M., *et al.*, 1996, *A&A*, 315, L165
- Peretto, N. & Fuller, G. A. 2009, *A&A*, 505, 405
- Peretto, N., *et al.*, 2010, *A&A*, 518, L98
- Pilbratt, G. L., *et al.*, 2010, *A&A*, 518, L1
- Pillai, T., Wyrowski, F., Carey, S. J., & Menten, K. M. 2006, *A&A*, 450, 569
- Pillai, T., Wyrowski, F., Hatchell, J., Gibb, A. G., & Thompson, M. A. 2007, *A&A*, 467, 207
- Pineda, J. E., Caselli, P., & Goodman, A. A. 2008, *ApJ*, 679, 481
- Pineda, J. E., Goodman, A. A., Arce, H. G., Caselli, P., Longmore, S., & Corder, S. 2011, *ApJ*, in press (arXiv:1106.5474)
- Poelman, D. R., Spaans, M., & Tielens, A. G. G. M. 2007, *A&A*, 464, 1023
- Ragan, S., Bergin, E., & Wilner, D. 2011, *ApJ*, in press (arXiv:1105.4182)
- Rathborne, J. M., Jackson, J. M., & Simon, R. 2006, *ApJ*, 641, 389
- Rathborne, J. M., Lada, C. J., Muench, A. A., Alves, J. F., Kainulainen, J., & Lombardi, M. 2009, *ApJ*, 699, 742
- Roberts, H., Herbst, E., & Millar, T. J. 2003, *ApJ*, 591, L41
- Salpeter, E. E. 1955, *ApJ*, 121, 161
- Schnee, S., Caselli, P., Goodman, A., Arce, H. G., Ballesteros-Paredes, J., & Kuchibhotla, K. 2007, *ApJ*, 671, 1839
- Shu, F. H., Adams, F. C., & Lizano, S. 1987, *ARAA*, 25, 23
- Stamatellos, D., Griffin, M. J., Kirk, J. M., Molinari, S., Sibthorpe, B., Ward-Thompson, D., Whitworth, A. P., & Wilcock, L. A. 2010, *MNRAS*, 409, 12
- Swift, J. J. 2009, *ApJ*, 705, 1456
- Tafalla, M., Myers, P. C., Caselli, P., & Walmsley, C. M. 2004, *A&A*, 416, 191
- Tafalla, M., Santiago-García, J., Myers, P. C., Caselli, P., Walmsley, C. M., & Crapsi, A. 2006, *A&A*, 455, 577
- Tan, J. C. 2000, *ApJ*, 536, 173
- Tan, J. C. 2005, *Cores to Clusters: Star Formation with Next Generation Telescopes*, 87
- Teyssier, D., Hennebelle, P., & Pérault, M. 2002, *A&A*, 382, 624
- Troscompt, N., Faure, A., Maret, S., Ceccarelli, C., Hily-Blant, P., & Wiesenfeld, L. 2009, *A&A*, 506, 1243
- van der Tak, F. F. S., Caselli, P., & Ceccarelli, C. 2005, *A&A*, 439, 195

- van der Tak, F. F. S., *et al.*, 2010, *A&A*, 518, L107
- van Dishoeck, E. F., Blake, G. A., Draine, B. T., & Lunine, J. I. 1993, *Protostars and Planets III*, 163
- van Dishoeck, E. F., *et al.*, 2011, *PASP*, 123, 138
- van Loo, S., Falle, S. A. E. G., Hartquist, T. W., & Moore, T. J. T. 2007, *A&A*, 471, 213
- Vastel, C., Caselli, P., Ceccarelli, C., Phillips, T., Wiedner, M. C., Peng, R., Houde, M., & Dominik, C. 2006, *ApJ*, 645, 1198
- Vasyunina, T., Linz, H., Henning, T., Zinchenko, I., Beuther, H., & Voronkov, M. 2011, *A&A*, 527, A88
- Vastel, C., Caux, E., Ceccarelli, C., Castets, A., Gry, C., & Baluteau, J. P. 2000, *A&A*, 357, 994
- Vastel, C., Phillips, T. G., & Yoshida, H. 2004, *ApJ*, 606, L127
- Walmsley, C. M., Flower, D. R., & Pineau des Forêts, G. 2004, *A&A*, 418, 1035
- Ward-Thompson, D., Motte, F., & Andre, P. 1999, *MNRAS*, 305, 143
- Ward-Thompson, D., Scott, P. F., Hills, R. E., & Andre, P. 1994, *MNRAS*, 268, 276
- Wilcock, L. A., *et al.*, 2011, *A&A*, 526, A159
- Willacy, K., Langer, W. D., & Velusamy, T. 1998, *ApJ*, 507, L171
- Zhang, Q., Wang, Y., Pillai, T., & Rathborne, J. 2009, *ApJ*, 696, 268
- Zhang, S. B., Yang, J., Xu, Y., Pandian, J. D., Menten, K. M., & Henkel, C. 2011, *ApJS*, 193, 10
- Zucconi, A., Walmsley, C. M., & Galli, D. 2001, *A&A*, 376, 650

Discussion

MELNICK: A note of caution... You refer to the abundance of H₂O, $x(\text{H}_2\text{O})$, in several contexts relating to pre-stellar cores. Because we believe that the gas-phase H₂O resides primarily in a relatively narrow zone near the cloud surface, dividing the inferred H₂O column density with that of any tracer that samples the bulk of the cloud volume, such as ¹³CO or dust, will result in an underestimate of $x(\text{H}_2\text{O})$.

CASELLI: This is true if models are indeed a good representation of reality. However, unlike model predictions, our recent Herschel observations toward L1544 suggest that H₂O must be present toward the center of the pre-stellar core (to produce the emission observed in the high sensitivity HRS spectrum) and not much toward the outskirts (to avoid total absorption). For L1544, we use the dust continuum emission to derive the H₂ column density and then compute $x(\text{H}_2\text{O})$. Chemical/dynamical models are then used to derive the abundance profile (Keto & Caselli 2010, with a chemistry based on Hollenbach *et al.* 2009). Our recent observations are consistent with an almost constant value of $x(\text{H}_2\text{O})$ (10^{-10} - 10^{-9}) across the core.

GOLDSMITH: How does the kinematic model explain the line profile of water observed in L1544?

CASELLI: What we see is the typical infall asymmetry also seen in other molecular transitions such as HCO⁺ (3-2) and CS(2-1), see e.g. Mardones *et al.* (1997) and Gregersen *et al.* (1997). The blue peak is coming from a region close to the center and behind the core nucleus. The gas in front of the core nucleus is redshifted because of the infall and the water line (with high critical density) is heavily self-absorbed. The absorption feature is below the continuum level set by dust emission at the frequency of the water line.

VAN DER TAK: Detection of para-H₂O towards L1544 may not be harder than ortho-H₂O because of the stronger dust continuum.

CASELLI: This is a very interesting suggestion and we will explore this more (although

preliminary calculations showed integration times quite large, it would be extremely important to uniquely measure the ortho/para ratio of H₂O in a quiescent source).

SEMENOV: The problems of chemical models of pre-stellar cores can in fact be the problem with physical models. For example, fractal structure of PSCs will enable much needed FUV-evaporation of ices in cloud cores. This may explain the need of having high H₂O abundances in the centers of PSCs.

CASELLI: This could indeed be the case, although so far VLA and PdBI data does not show evidence of fractal structure. Besides, the scenario you propose may also enhance the abundance of water in the envelope, and this is against what we observe. However, ALMA will shed light on the small scale structure of PSCs and definitely help to more quantitatively answer your question.